

Photospheric carbon, nitrogen, and oxygen abundances of A-type main-sequence stars *

Yoichi TAKEDA,^{1,2} Satoshi KAWANOMOTO,¹ Naoko OHISHI,¹
Dong-Il KANG,³ Byeong-Cheol LEE,^{4,5} Kang-Min KIM,^{4,5} and Inwoo HAN^{4,5}
¹National Astronomical Observatory, 2-21-1 Osawa, Mitaka, Tokyo 181-8588, Japan
takeda.yoichi@nao.ac.jp, kawanomoto.satoshi@nao.ac.jp, naoko.ohishi@nao.ac.jp

²SOKENDAI, The Graduate University for Advanced Studies, 2-21-1 Osawa, Mitaka, Tokyo 181-8588

³Changwon Science high school, 30, Pyungsanro 159-th, Uichang, Changwon, 641-500, Korea
kangdongil@gmail.com

⁴Korea Astronomy and Space Science Institute, 776, Daedeokdae-Ro, Yuseong-Gu, Daejeon 34055, Korea
bclee@kasi.re.kr, kmkim@kasi.re.kr, iwhan@kasi.re.kr

⁵Korea University of Science and Technology, 217, Gajeong-ro Yuseong-gu, Daejeon 34113, Korea

(Received 2018 May 2; accepted 2018 July 16)

Abstract

Based on the spectrum fitting method applied to C I 5380, N I 7486, and O I 6156–8 lines, we determined the abundances of C, N, and O for 100 mostly A-type main-sequence stars (late B through early F at $11000 \text{ K} \gtrsim T_{\text{eff}} \gtrsim 7000 \text{ K}$) comprising normal stars as well as non-magnetic chemically peculiar (CP) stars in the projected rotational velocity range of $0 \text{ km s}^{-1} \lesssim v_e \sin i \lesssim 100 \text{ km s}^{-1}$, where our aim was to investigate the abundance anomalies of these elements in terms of mutual correlation, dependence upon stellar parameters, and difference between normal and CP stars. We found that CNO are generally underabundant (relative to the standard star Procyon) typically by several tenths dex to ~ 1 dex for almost all stars (regardless of CP or normal), though those classified as peculiar (Am or HgMn) tend to show larger underabundance, especially for C in late Am stars and for N in HgMn stars of late B-type, for which deficiency amounts even up to ~ 2 dex. While the behaviors of these three elements are qualitatively similar to each other, the quantitative extent of peculiarity (or the vulnerability to the physical process causing anomaly) tends to follow the inequality relation of $C > N > O$. Regarding the considerable star-to-star dispersion observed at any T_{eff} , the most important cause is presumably the difference in rotational velocity. These observational facts appear to be more or less favorably compared with the recent theoretical calculations based on the model of atomic diffusion and envelope mixing.

Key words: physical processes: diffusion — stars: abundances
— stars: atmospheres — stars: chemically peculiar — stars: early-type

1. Introduction

It has long been known that a fraction of stars in the upper main sequence around A-type show unusual spectra characterized by conspicuous strengthening of specific metallic lines (or weakening of some lines such as Ca II K), indicating that the abundances of relevant elements are anomalous in their atmosphere. These stars are thus called “chemically peculiar stars” (CP stars), which are further divided into several subclasses (e.g., Preston 1974). Since the notable property of these CP stars that they are generally sharp-lined and thus rotate more slowly in comparison with normal stars, slow rotation is considered to be the important factor for producing abundance anomalies. Theoretically, the most promising mechanism for the origin of such chemical peculiarity is “atomic diffusion”; i.e., a kind of element segregation process caused by

imbalance between the downward gravitational force and the upward radiative force, which effectively acts when the atmosphere/envelope is sufficiently stable to prevent from substantial mixing (see, e.g., Michaud, Alecian, & Richer 2015; and the references therein). In this scenario, slow rotation is regarded as a necessary condition to guarantee the stability required for the build-up of anomaly.

Among the elements involved in CP phenomena, the light elements C, N, and O (which are most abundant next to H and He and thus of profound astrophysical importance) exhibit rather unique characteristics, in the sense that they show deficiencies unlike many other heavier species tending to suffer overabundances, because upward radiative acceleration is not so large as to counter the downward gravity acceleration (e.g., Gonzalez, Artru, & Michaud 1995). However, since the equilibrium surface abundances are eventually determined by how the hydrodynamical mixing process (e.g., meridional circulation, turbulence, mass loss, etc.) actually operates in the stellar envelope or atmosphere, the theoretical prediction heavily depends on the modeling details (e.g., how

* Based on observations carried out at Okayama Astrophysical Observatory (National Astronomical Observatory of Japan) and Bohyunsan Astronomical Observatory (Korean Astronomy and Space Science Institute).

the mixing-related parameters are chosen), the validity of which has to be empirically checked in comparison with observations.

Unfortunately, previous observational studies of CNO abundances in A-type stars are not necessarily satisfactory in this respect, despite that a large number of spectroscopic investigations on the chemical abundances of CP and normal A stars have been published so far.

— First, the size and diversity of the sample is generally not sufficient, because such spectroscopic study published in a paper usually targets only a comparatively small number of stars. Moreover, they tend to be biased toward sharp-line stars of small $v_e \sin i$ (projected rotational velocity) because of the increasing difficulty in analyzing the spectra of broad-line stars. In order to provide useful observational constraints for theoretical modeling of atomic diffusion, sample stars are desired to cover a wide range of relevant stellar parameters, which are considered to affect the prediction of surface abundance peculiarity (e.g., $v_e \sin i$, T_{eff}).

— Second, although a number of previous investigations (e.g., Fossati et al. 2007, 2009; Royer et al. 2014; and the references therein) included any of CNO (especially C or O) along with various other elements, only a few have focused on consistently studying the abundances for all the three in A-type stars and comparing them with each other (e.g., Roby & Lambert 1990; Leushin et al. 1992; Savanov 1995). Actually, the pioneering work by Roby and Lambert (1990), who studied the CNO abundances of 37 CP stars and 5 standard A and late-B stars, still remains as the most widely quoted study in this field. Especially, information of N abundances for such A-type and related stars is evidently insufficient, presumably because N lines generally suffer considerable non-LTE effect (Takeda 1992b; Rentsch-Holm 1996; Lemke & Venn 1996; Przybilla & Butler 2001). This situation should be redressed by all means.

Motivated by this circumstance, we decided to conduct a comprehensive study on the abundances of C, N, and O for a large sample of 100 late-B through early-F stars (including not only CP stars but also normal stars) covering sufficiently large ranges of stellar parameters ($11000 \text{ K} \gtrsim T_{\text{eff}} \gtrsim 7000 \text{ K}$ and $0 \text{ km s}^{-1} \lesssim v_e \sin i \lesssim 100 \text{ km s}^{-1}$), where the synthetic spectrum-fitting method was applied (inevitable for analyzing the spectra of broad-line stars) and the non-LTE effect was properly taken into consideration. This is kind of an extension of our previous work (Takeda et al. 2008, 2009; hereinafter referred to as T08 and T09, respectively), in which C or O were included as target elements), but the sample has been considerably refined by adding new observational data and attention has been paid also to N. The points of interest which we want to clarify are as follows:

- Do the abundance trends of these three elements correlate well with each other? Or do they show any notable difference? What about their relation to the metallicity (Fe)?
- How do the extents of peculiarity in C, N, and O de-

pend upon the stellar parameters? Can we observe any dependence upon $v_e \sin i$ or T_{eff} ?

- Are there any distinct difference between CP stars and normal stars in terms of CNO abundances? Do stars classified as normal exhibit any sign of chemical peculiarity?

2. Observational data

Given the spectral data of a large number of stars of B–A–F types currently available to us (either the data already used in our previous studies or newly observed data), we selected our target sample by considering the following requirements:

— As one of our main aims was to examine the effect of stellar rotation on CNO abundance peculiarities, we would like to include stars in as wide $v_e \sin i$ range as possible. However, according to our experience (T08, T09), abundance determination for very rapid rotators (e.g., $v_e \sin i \sim 200\text{--}300 \text{ km s}^{-1}$) is not easy and often fails, while our spectrum-fitting approach turned out successful for most stars of $v_e \sin i \lesssim 100 \text{ km s}^{-1}$. Since Abt and Morrell (1995) reported that abundance anomalies are seen mostly for stars with $v_e \sin i$ lower than $\sim 120 \text{ km s}^{-1}$, we decided to confine our targets only to those of $v_e \sin i \leq 100 \text{ km s}^{-1}$.

— Although our main emphasis is placed on A-type stars, they had better be discussed in company with early-F stars (where Am-like anomaly is also observed) and late-B stars (where HgMn peculiarity is seen), which are considered to be closely related.

— Among the various types of CP stars on the upper main sequence, we already learned that spectra of magnetic CP stars (in which variability is often involved) tend to be so complex that they can not be well fitted by the conventional spectrum modeling. Therefore, we concentrated only on non-magnetic CP stars (Am stars or HgMn stars). — In order to investigate the cause of abundance peculiarity, studying a sufficient number of cluster stars altogether is useful, because they should have been born with the same initial composition. For this purpose, we included A–F stars belonging to the Hyades cluster.

Consequently, our program stars consist of 100 mostly A-type stars (late B through early F) on or near to the main sequence (luminosity classes of III–V) which have slow to moderately-high rotational velocities ($0 \text{ km s}^{-1} \lesssim v_e \sin i \lesssim 100 \text{ km s}^{-1}$). Among these, about $\sim 30\%$ are non-magnetic CP stars: 25 Am stars (from the spectral type given in the Hipparcos catalogue; cf. ESA 1997) and 5 HgMn (or Mn) stars (cf. table 1 of Takeda et al. 1999). Besides, 16 stars (about $\sim 1/6$) are Hyades stars. The list of these program stars is given in table 1. It may be worth noting that a significant fraction of our targets are spectroscopic binaries (data taken from Hoffleit & Jaschek 1991), for which the high binary frequency in Am stars (cf. Preston 1974) may be at least partially responsible. However, apparently doubled-lined binaries (such as those difficult to be modeled by the theoretical spectrum simulated for a single star) are not included in our sample stars.

Regarding the observational data, we could avail ourselves of the spectra already at our hand for 71 stars and the standard star Procyon, which were used in our previous studies, as summarized in table 2. Meanwhile, the data of 29 stars were secured by our new observations carried out on 2017 August 22–23 and November 6 by using the 188 cm reflector along with HIDES (High Dispersion Echelle Spectrograph) at Okayama Astrophysical Observatory. The data reduction was done in the standard manner by using IRAF,¹ which resulted in spectra with the resolving power of $R \sim 100000$ covering the wavelength range of 5100–8800 Å. For most of the spectra of our 100 targets, sufficiently high S/N ratios (typically on the order of ~ 200) are attained.

3. Stellar parameters and model atmospheres

As in our previous studies (see the references given in table 2), the effective temperature (T_{eff}) and the surface gravity ($\log g$) for each of the 100 program stars were determined from the colors of Strömberg’s *uvby*β photometric system with the help of Napiwotzki, Schönberner, and Wenske’s (1993) *uvbybetanew* program², where the observational data of $b - y$, c_1 , m_1 , and β were taken from Hauck and Mermilliod (1998) via the SIMBAD database. Their typical errors may be on the order of $\sim 3\%$ in T_{eff} and ~ 0.1 dex in $\log g$ for the present case of stars around A-type (cf. Sect. 5 of Napiwotzki et al. 1993). Regarding the microturbulence (v_t), we adopted the analytical T_{eff} -dependent relation derived in T08

$$v_t = 4.0 \exp\{-[\log(T_{\text{eff}}/8000)/A]^2\} \quad (1)$$

(where $A \equiv [\log(10000/8000)]/\sqrt{\ln 2}$), which roughly represents the observed distribution of v_t with probable uncertainties of $\pm 30\%$ (cf. Fig. 2b in T08). The only exception is the standard star Procyon, for which we used Takeda et al.’s (2005b) spectroscopically determined values ($T_{\text{eff}} = 6612$ K, $\log g = 4.00$, and $v_t = 2.0$ km s⁻¹) in order to maintain consistency with T08. The adopted values of T_{eff} , $\log g$, v_t are summarized in table 1. All the program stars are plotted on the $\log L$ vs. $\log T_{\text{eff}}$ diagram (theoretical HR diagram) in figure 1, where seven representative theoretical evolutionary tracks corresponding to different stellar masses are also depicted. We can see from this figure that the masses of our sample stars are in the range between $\sim 1.5M_{\odot}$ and $\sim 5M_{\odot}$. More detailed data regarding the targets and their stellar parameters are given in the electronic table (tableE.dat) presented as the online material.

The model atmosphere for each star was then constructed by two-dimensionally interpolating Kurucz’s (1993) ATLAS9 model grid (for $v_t = 2$ km s⁻¹) in terms of T_{eff} and $\log g$, where the solar-metallicity models were exclusively used as in our previous studies. We also com-

puted the non-LTE departure coefficients for C, N, and O corresponding to each atmospheric model, which are to be used for non-LTE abundance analysis, by following the procedure described in Takeda (1992b) (for C and N) and Takeda (1992a, 2003) for O.

4. Determination of CNO abundances

Following our previous studies, we invoke the C I 5380.337 line (as in T08) and the O I 6156–8 feature comprising 9 components (as in T08, T09, Takeda et al. 2012, 2014) for deriving the C and O abundances. As to N, we decided to adopt the N I line at 7468.312 Å, which has a suitable strength as an abundance indicator. The determination procedures of abundances and related quantities (e.g., non-LTE correction, uncertainties due to ambiguities of atmospheric parameters) are essentially the same as in our previous papers quoted above, which consist of two consecutive steps.

4.1. Synthetic spectrum fitting

The first step is to find the solutions for the abundances of relevant elements (A_1, A_2, \dots), projected rotational velocity ($v_e \sin i$), and radial velocity (V_{rad}) such as those accomplishing the best fit (minimizing $O - C$ residuals) between theoretical and observed spectra, while applying the automatic fitting algorithm (Takeda 1995). Three wavelength regions were selected for this purpose: (1) 5375–5390 Å region (for C), (2) 7457–7472 Å region (for N), and (3) 6146–6163 Å region (for O). More information about this fitting analysis (varied elemental abundances, used data of atomic lines) is summarized in table 3. How the theoretical spectrum for the converged solutions fits well with the observed spectrum is displayed in figures 2–4 for each region. The $v_e \sin i$ values³ resulting from the fitting of 6146–6163 Å region are presented in table 1. We also adopted the solution of Fe abundance derived from the fitting of 6146–6163 Å region as the metallicity of each star (given as [Fe/H] in table 1).

4.2. Abundances from equivalent widths

As the second step, with the help of Kurucz’s (1993) WIDTH9 program (which had been considerably modified in various respects; e.g., inclusion of non-LTE effects, treatment of total equivalent width for multi-component lines; etc.), we computed the equivalent widths (W) of the representative lines “inversely” from the abundance solutions (resulting from spectrum synthesis) along with the adopted atmospheric model/parameters; i.e., W_{5380} (for C I 5380), W_{6156-8} (for O I 6156–8), and W_{7468} (for N I 7468), because they are easier to handle in practice (e.g., for estimating the uncertainty due to errors in

¹ IRAF is distributed by the National Optical Astronomy Observatories, which is operated by the Association of Universities for Research in Astronomy, Inc. under cooperative agreement with the National Science Foundation.

² <http://www.astro.le.ac.uk/~rn38/uvbybeta.html>.

³ It should be kept in mind that we assumed only the rotational broadening (with the limb-darkening coefficient of $\epsilon = 0.5$) as the macrobroadening function to be convolved with the intrinsic theoretical line profiles. Accordingly, $v_e \sin i$ values for very sharp-line cases (e.g., $v_e \sin i \lesssim 5-6$ km s⁻¹) should be regarded rather as upper limits because the effects of instrumental broadening and macroturbulence are neglected.

atmospheric parameters). The adopted atomic data for these lines are summarized in table 4. We then analyzed such derived W values by using WIDTH9 to determine A^N (NLTE abundance) and A^L (LTE abundance), from which the NLTE correction $\Delta(\equiv A^N - A^L)$ was further derived. Since we adopted Procyon as the standard star of abundance reference, which is known to have essentially the same abundance as the Sun (cf. Sect. IV(c) in T08; see also Takeda 1994), we define the relative abundance as $[X/H] \equiv A_X^N(\text{star}) - A_X^N(\text{Procyon})$ ($X = \text{C, N, O}$). The resulting values of $[C/H]$, $[N/H]$, and $[O/H]$ are given in table 1 (more complete results including W and Δ are separately presented in “tableE.dat”). Figures 5(C), 6(N), and 7(O) graphically show the equivalent width (W), non-LTE correction (Δ), non-LTE abundance (A^N), and abundance variations in response to parameter changes (see the following subsection 4.3), as functions of T_{eff} . As we can recognize in panel (b) of these figures, while the non-LTE corrections for C I 5380 and O I 6156–8 are not very significant ($|\Delta| \lesssim 0.1$ dex), those for N I 7486 are rather important (up to $|\Delta| \lesssim 0.4\text{--}0.5$ dex) and thus have to be taken into consideration especially at higher T_{eff} .

4.3. Error estimation

In order to evaluate the abundance errors caused by uncertainties in atmospheric parameters, we estimated six kinds of abundance variations (δ_{T+} , δ_{T-} , δ_{g+} , δ_{g-} , δ_{v+} , and δ_{v-}) for A^N by repeating the analysis on the W values while perturbing the standard atmospheric parameters interchangeably by $\pm 3\%$ in T_{eff} , ± 0.1 dex in $\log g$, and $\pm 30\%$ in v_t (which are the typical ambiguities of the parameters we adopted; cf. section 3). Finally, the root-sum-square of these perturbations, $\delta_{Tgv} \equiv (\delta_T^2 + \delta_g^2 + \delta_v^2)^{1/2}$, were regarded as abundance uncertainties (due to combined errors in T_{eff} , $\log g$, and v_t), where δ_T , δ_g , and δ_v are defined as $\delta_T \equiv (|\delta_{T+}| + |\delta_{T-}|)/2$, $\delta_g \equiv (|\delta_{g+}| + |\delta_{g-}|)/2$, and $\delta_v \equiv (|\delta_{v+}| + |\delta_{v-}|)/2$, respectively. These $\delta_{T\pm}$, $\delta_{g\pm}$, and $\delta_{v\pm}$ are plotted against T_{eff} in panels (d), (e), and (f) of figures 5–7. We can see that only $\delta_{T\pm}$ can be appreciably significant ($\lesssim 0.1\text{--}0.2$ dex) reflecting the high-excitation nature of the adopted lines, while $\delta_{g\pm}$ and $\delta_{v\pm}$ are of negligible importance (insensitivity to changing v_t is interpreted as due to the large thermal velocity for these light elements).

We also evaluated errors due to random noises of the observed spectra by estimating S/N-related uncertainties in the equivalent width (W) by invoking the relation derived by Cayrel (1988), $\delta W \simeq 1.6(w\delta x)^{1/2}\epsilon$, where δx is the pixel size (0.03 Å), w is the full-width at half maximum (which may be roughly regarded as $\sim \lambda v_e \sin i/c$; where λ is line wavelength and c is the velocity of light), and $\epsilon \equiv (S/N)^{-1}$; typically $\sim 1/200$). Then, we determined the abundances for each of the perturbed $W_+(\equiv W + \delta W)$ and $W_-(\equiv W - \delta W)$, from which the differences from the standard abundance (A) were derived as $\delta_{W+}(> 0)$ and $\delta_{W-}(< 0)$. We thus regard $\delta_W \equiv 0.5(\delta_{W+} + |\delta_{W-}|)$ as the abundance uncertainties due to photometric noises.

Since the equivalent width error (δW) is in the range of only $\sim 0.3\text{--}2$ mÅ, the corresponding abundance ambiguity (δ_W) is generally insignificant (on the order of a few hundredths dex in most cases).

Exceptionally, however, in case of very weak lines, δ_W can be appreciably large as much as several tenths dex. As a tentative criterion, we regard that the resulting abundance is unreliable if W is smaller than $3\delta_W$.⁴ We then found that 11 $[C/H]$ values and 4 $[N/H]$ values (none of the $[O/H]$ values) satisfy this condition, which are thus unreliable and should be viewed with caution. Practically, they had better be regarded rather as upper limits. These results of large uncertainties are shown with parentheses in table 1, and the relevant plots are marked by open circles in figure 5a,c and figure 6a,c.

Finally, combining δ_{Tgv} and δ_W , we obtained the total error as $\delta_{TgvW} \equiv (\delta_{Tgv}^2 + \delta_W^2)^{1/2}$, which are shown as error bars attached to the non-LTE abundances in panel (b) of figures 5–7. According the characteristics mentioned above, δ_{TgvW} is generally dominated by δ_{Tgv} (i.e., $\delta_{TgvW} \simeq \delta_{Tgv}$), excepting the cases of very weak lines where δ_W begins to show appreciable/dominant contribution. The detailed values of δ_{Tgv} , δ_W , and δ_{TgvW} for each star are given in “tableE.dat” (available as online material).

5. Discussion

5.1. Observed behaviors of $[C/H]$, $[N/H]$, and $[O/H]$

The relative abundances ($[C/H]$, $[N/H]$, $[O/H]$, and $[Fe/H]$) for each star resulting from our analysis in section 4 are plotted against T_{eff} and $v_e \sin i$ in figure 8 (panels a–h), where their mutual correlations are also shown (panels i–n). The following characteristics can be read from these figures.

— C, N, and O are underabundant for almost all program stars (regardless of whether being classified as peculiar or normal, though larger anomaly tends to be seen in the former) typically by several tenths dex to ~ 1 dex ($-1 \lesssim [C,N,O/H] \lesssim 0$), in contrast to $[Fe/H]$ distributing around $[Fe/H] \sim 0$.

— Moreover, with regard to $[C/H]$ and $[N/H]$, distinctly large deficiencies as much as ~ 2 dex are shown by a fraction of stars, most of which are CP stars. That is, especially large depletion is observed in $[C/H]$ for late Am stars ($T_{\text{eff}} \sim 7500\text{--}8000$ K; cf. figure 8e) or in $[N/H]$ for HgMn stars ($T_{\text{eff}} \sim 10000\text{--}11000$ K; cf. figure 8f).

— When the extents of peculiarity (deficiency) for these three elements are compared with each other, we may state that (if the conspicuously C- or N-depleted stars mentioned above are excluded) the inequality relation $|[C/H]| > |[N/H]| > |[O/H]|$ roughly holds. In other words, carbon is more sensitive than nitrogen and nitrogen is more sensitive than oxygen to the mechanism of producing the anomaly. It is interesting to note that this is consis-

⁴ We can use W_{5380} and W_{7648} for W as it is. However, since W_{6156-8} is the combined equivalent width of the feature apparently seen as a triplet (cf. table 4), we substituted $W_{6156-8}/3$ for W .

tent with what has been predicted from the diffusion theory (see, e.g., Figs. 12–13 of Richer, Michaud, & Turcotte 2000; Figs. 14–16 of Talon, Richard, & Michaud 2006).

— Regarding the connection between the CNO abundances and the metallicity ($[\text{Fe}/\text{H}]$), we can see a trend of anti-correlation; i.e., $[\text{C}/\text{H}]$, $[\text{N}/\text{H}]$, and $[\text{O}/\text{H}]$ tend to decrease with an increase in $[\text{Fe}/\text{H}]$ (cf. figure 8i, 8j, and 8k). This indicates that the sense of chemical anomaly acts oppositely for CNO and heavier metals (cf. section 1).

5.2. Dependence upon Stellar Parameters

Then, which parameter is most important in determining the extent of peculiarity? The $v_e \sin i$ -dependence of $[\text{C}/\text{H}]$, $[\text{N}/\text{H}]$, and $[\text{O}/\text{H}]$, which is expected if the mechanism of atomic diffusion (countervailing the rotation-dependent mixing) is the main cause for the CP phenomenon, is not necessarily clear in figures 8a, 8b, and 8c. However, this is presumably due to the diversity of the sample stars (difference of initial composition, etc.). In figure 9 are shown the same correlation plots as figure 8 but only for the selected 16 Hyades stars. We can see from this figure more manifestly that $[\text{C}/\text{H}]$, $[\text{N}/\text{H}]$, and $[\text{O}/\text{H}]$ progressively decrease with a decrease in $v_e \sin i$ from ~ 0 (at $v_e \sin i \sim 100 \text{ km s}^{-1}$) to ~ -1 (at $v_e \sin i \sim 0 \text{ km s}^{-1}$). Similarly to the case of figure 8 mentioned in subsection 5.1, we can recognize (much more clearly) the mutual correlation between C, N, and O with the inequality relation of $||[\text{C}/\text{H}]| > |[\text{N}/\text{H}]| \gtrsim |[\text{O}/\text{H}]|$ (cf. panels l, m, and n in figure 9) in this homogeneous sample. Actually, Takeda and Sadakane (1997) already reported the existence of such trend in Hyades stars for oxygen based on the analysis of O I 7771–5 triplet lines. This time, we have confirmed this tendency not only for O but also for C and N. It should also be noted that Gebran et al. (2010) reported the tendency of anticorrelation in $[\text{C}/\text{H}]$ vs. $[\text{Fe}/\text{H}]$ as well as $[\text{O}/\text{H}]$ vs. $[\text{Fe}/\text{H}]$ plots (i.e., close correlation between $[\text{C}/\text{H}]$ and $[\text{O}/\text{H}]$) for Hyades A–F dwarfs (cf. their Fig. 8) similar to our figures 9i and 9k.

From theoretical point of view, the diffusion model for the explanation of AmFm peculiarity predicts a T_{eff} -dependent tendency; i.e., the extent of CNO deficiency progressively increases with decreasing T_{eff} (e.g., figure 14 of Richer et al. 2000). Interestingly, we can recognize such a trend in figures 8e–8g (and also in figures 9e–9g despite the rather narrow T_{eff} range of $\sim 9000\text{--}7000 \text{ K}$) for the combined sample⁵ of Am stars (red-filled symbols) and normal stars (open symbols). That is, the dispersion of $[\text{X}/\text{H}]$ ($\text{X} = \text{C}, \text{N}, \text{O}$) grows and the lower envelope of the distribution shifts toward lower values with a decrease in T_{eff} . This may be regarded as being in support of the recent theoretical models at least in the qualitative sense.

5.3. Comparison with previous work

Finally, we comment on the comparison of our results with several published studies mentioned in section 1.

— Roby and Lambert (1990) determined the CNO abun-

dances of 13 Am stars, 9 HgMn stars, and 5 normal (standard) stars in the T_{eff} range of $\sim 7000\text{--}15000 \text{ K}$, where most of the sample stars are sharp-lined with $v_e \sin i \lesssim 50 \text{ km s}^{-1}$. They reported that the mean (C, N, O) abundances of Am stars and HgMn stars relative to standard stars to be $(-0.2, -0.2, -0.4)$ dex and $(+0.1, -0.7, -0.3)$ dex. Although these extents of deficiency appear somewhat small compared to ours, we should bear in mind that normal stars are not guaranteed to have solar CNO composition, as revealed from this study. When we examine the absolute abundances (relative to the solar abundances) shown in their Fig. 1 (standard stars), Fig 2 (HgMn stars), and Fig. 5 (Am stars), their results are favorably compared with our figures 8e–8g in the sense that normal stars show marginal underabundances by $\sim 0.0\text{--}0.3$ dex, CNO deficiencies of Am stars have rather large dispersion ($\sim 0.0\text{--}1.0$ dex), and HgMn stars exhibit moderate underabundance (by several tenths dex) in C and O along with considerably large deficit ($\gtrsim 1$ dex) in N.

— Regarding Leushin et al.’s (1992) analysis on CNO abundances of CP stars, 5 among their 7 targets are of Si or SrCrEu type (magnetic CP stars which are not touched in our study) and 2 are HgMn stars. Only C lines were measured for these two HgMn stars to yield $[\text{C}/\text{H}] \sim -0.4$ dex (reasonably consistent with our consequence), while N lines were too weak to be measurable (O lines were not measured for these stars).

— Savanov (1995) investigated the correlation between the CNO and Fe abundances of CP stars and normal stars, based on the already published abundance data taken from various literature. He reported that $[\text{C}/\text{H}]$, $[\text{N}/\text{H}]$, and $[\text{O}/\text{H}]$ are anti-correlated with $[\text{Fe}/\text{H}]$ (this tendency is still recognized even by excluding the weak-line λ Boo stars of low $[\text{Fe}/\text{H}]$, which are out of the scope in this study), such as we confirmed in figures 8i–8k and figures 9i–9k.

— Fossati et al. (2007) determined chemical abundances of many elements for 8 Am stars in the Praesepe cluster (along with 2 normal A-type stars and 1 Blue-Straggler). We see from their Fig. 10 that two normal A-type stars ($T_{\text{eff}} \sim 7400\text{--}7800 \text{ K}$) show $[\text{C}/\text{H}] \sim 0.0$, $[\text{N}/\text{H}] \sim +0.5$, and $[\text{O}/\text{H}] \sim +0.1$ on the average. Regarding Am stars ($T_{\text{eff}} \sim 7200\text{--}8500 \text{ K}$), the abundance ranges are: $[\text{C}/\text{H}] \sim -0.7$ to 0.0 , $[\text{N}/\text{H}] \sim -0.4$ to -0.2 (with an exceptionally large value of $\sim +0.4$ for HD 72942), and $[\text{O}/\text{H}] \sim -0.6$ to -0.2 . Although the general tendency of CNO deficiency for Am stars are surely observed, it appears that their abundances are somewhat higher than our results (especially for N), which may be due to their neglect of non-LTE corrections.

— Fossati et al. (2009) carried out elaborate chemical abundance studies for 3 sharp-lined normal early-A and late-B stars (HD 145788, 21 Peg, and π Cet, which have T_{eff} of 9750, 10400, and 12800 K, respectively). Their LTE results show that $[\text{C}/\text{H}]$, $[\text{N}/\text{H}]$, and $[\text{O}/\text{H}]$ for these stars are generally supersolar (> 0) by a few tenths dex (cf. their Fig. 7), which is not consistent with our conclusion that even normal stars show some deficits in CNO. Again, this may indicate that non-LTE effect should be

⁵ The $[\text{N}/\text{H}]$ values in HgMn stars of higher T_{eff} are exceptional and should be separately considered, which show conspicuously large deficiencies.

adequately taken into account for deriving the abundances of such light elements (as they also discussed in Sect. 4.1.2 therein).

— Royer et al. (2014) determined the abundances of 14 chemical species for a homogeneous sample of 47 A0–A1 stars of comparatively low $v_e \sin i$ ($< 65 \text{ km s}^{-1}$). Comparing our $[\text{C}/\text{H}]$ and $[\text{O}/\text{H}]$ values with their results for 9 stars in common (cf. their Table 4), we can confirm a reasonable agreement within the error bars; i.e., the mean differences (ours–theirs) are $\langle \Delta[\text{C}/\text{H}] \rangle = -0.08$ (with the standard deviation of $\sigma = 0.08$) and $\langle \Delta[\text{O}/\text{H}] \rangle = -0.02$ ($\sigma = 0.11$). According to their Fig. 10 (abundance range seen from the box size corresponding to the width of distribution), the results for $[\text{C}/\text{H}]$ are ~ -0.2 to -0.5 (normal stars) and ~ -0.4 to -0.7 (CP stars) and those for $[\text{O}/\text{H}]$ are ~ 0.0 to -0.2 (normal stars) and ~ -0.2 to -0.4 (CP stars). We may state that these values are roughly consistent with our results for stars of $T_{\text{eff}} \sim 9000\text{--}11000 \text{ K}$ (see figures 8e–8g).

6. Conclusion

Despite that many studies have been published regarding the photospheric chemical abundances in normal and chemically-peculiar A-type stars on the upper main sequence, only a limited number of spectroscopic investigations have been carried out so far concerning their abundances of CNO (light elements of astrophysical importance), which are known to be generally deficient in CP stars in contrast to many other heavier elements tending to be overabundant.

Motivated by this situation, we conducted a comprehensive spectroscopic study on the abundances of C, N, and O for 100 main-sequence stars of mostly A-type (late B through early F at $11000 \text{ K} \gtrsim T_{\text{eff}} \gtrsim 7000 \text{ K}$) comprising normal stars as well as non-magnetic CP stars (Am and HgMn stars) in the projected rotational velocity range of $0 \text{ km s}^{-1} \lesssim v_e \sin i \lesssim 100 \text{ km s}^{-1}$, based on the high-dispersion spectra obtained at Okayama Astrophysical Observatory (new observation for 29 targets) and Bohyunsan Astronomical Observatory.

Our aim was to investigate the abundance anomalies of CNO from qualitative as well as quantitative point of view, especially in terms of their mutual correlation or correlation with Fe, dependence upon stellar parameters (T_{eff} , $v_e \sin i$), and difference between normal and CP stars.

Regarding the method of analysis, we applied the spectrum-fitting technique to C I 5380, N I 7486, and O I 6156–8 lines and evaluated their equivalent widths, from which the non-LTE abundances, non-LTE corrections, and sensitivities to perturbations in atmospheric parameters were derived.

The results of our analysis revealed the following observational characteristics regarding the CNO abundances of our sample stars:

- C, N, and O are underabundant for almost all cases (irrespective of a star is classified as peculiar or normal, though with a tendency of larger

anomaly for the former) typically in the range of $-1 \lesssim [\text{C,N,O}/\text{H}] \lesssim 0$, in contrast to $[\text{Fe}/\text{H}]$ distributing around $[\text{Fe}/\text{H}] \sim 0$.

- Moreover, distinctly large deficiencies as much as ~ 2 dex are shown for C or N by some CP stars ($[\text{C}/\text{H}]$ for late Am stars or $[\text{N}/\text{H}]$ for HgMn stars of late B-type)
- The inequality relation $|[\text{C}/\text{H}]| > |[\text{N}/\text{H}]| > |[\text{O}/\text{H}]|$ appears to roughly hold regarding the typical extents of anomaly (deficiency), which is consistent with the prediction from the recent model of atomic diffusion.
- We confirmed that $[\text{C}/\text{H}]$, $[\text{N}/\text{H}]$, and $[\text{O}/\text{H}]$ are anti-correlated with $[\text{Fe}/\text{H}]$, which means that the sense of chemical anomaly acts oppositely for CNO and heavier metals.
- The extent of CNO abundance peculiarity (deficiency) tends to be larger for lower $v_e \sin i$, which becomes especially manifest when we pay attention only to 16 Hyades stars of the same primordial composition. This may be in favor of the atomic diffusion theory for the cause of chemical anomaly, which would not work in the existence of efficient mixing by rapid rotation.
- In addition, the dispersion of $[\text{C}/\text{H}]$, $[\text{N}/\text{H}]$, and $[\text{O}/\text{H}]$ tends to grow (with the lower envelope of the distribution shifting toward lower values) with a decrease in T_{eff} , which is consistent with recent diffusion model predicting that the extent of CNO deficiency increases with decreasing T_{eff} .

This research has made use of the SIMBAD database, operated at CDS, Strasbourg, France. Data reduction was in part carried out by using the common-use data analysis computer system at the Astronomy Data Center (ADC) of the National Astronomical Observatory of Japan.

References

- Abt, H. A., & Morrell, N. I. 1995, *ApJS*, 99, 135
- Allende Prieto, C., Barklem, P. S., Lambert, D. L., & Cunha, K. 2004, *A&A*, 420, 183
- Arenou, F., Grenon, M., & Gómez, A. 1992, *A&A*, 258, 104
- Cayrel, R. 1988, in *The Impact of Very High S/N Spectroscopy on Stellar Physics*, Proc. IAU Symp. 132, eds. G. Cayrel de Strobel & M. Spite (IAU), p. 345
- ESA 1997, *The Hipparcos and Tycho Catalogues*, ESA SP-1200, available from NASA-ADC or CDS in a machine-readable form (file name: hip_main.dat)
- Flower, P. J. 1996, *ApJ*, 469, 355
- Fossati, L., Bagnulo, S., Monier, R., Khan, S. A., Kochukhov, O., Landstreet, J., Wade, G., & Weiss, W. 2007, *A&A*, 476, 911
- Fossati, L., Ryabchikova, T., Bagnulo, S., Alecian, E., Grunhut, J., Kochukhov, O., & Wade, G. 2009, *A&A*, 503, 945
- Gebran, M., Vick, M., Monier, R., & Fossati, L. 2010, *A&A*, 523, A71
- Gonzalez, J.-F., Artru, M.-C., & Michaud, G. 1995, *A&A*, 302, 788

- Hauck, B., & Mermilliod, M. 1998, *A&AS*, 129, 431
- Hoffleit, D., & Jaschek, C. 1991, *The Bright Star Catalogue*, 5th revised ed. (New Haven, Conn.: Yale University Observatory)
- Kurucz, R. L. 1993, Kurucz CD-ROM, No. 13 (Harvard-Smithsonian Center for Astrophysics)
- Kurucz, R. L., & Bell, B. 1995, Kurucz CD-ROM, No. 23 (Harvard-Smithsonian Center for Astrophysics)
- Lejeune, T., & Schaerer, D. 2001, *A&A*, 366, 538
- Lemke, M., & Venn, K. A. 1996, *A&A*, 309, 558
- Leushin, V. V., Ryabchikova, T. A., Topil'skaya, G. P., & Pavlova, V. M. 1992, *Sov. Astron.* 36, 279
- Michaud, G., Alecian, G., & Richer, J. 2015, in *Atomic Diffusion in Stars* (Switzerland: Springer International Publishing)
- Napiwotzki, R., Schönberner, D., & Wenske, V. 1993, *A&A*, 268, 653
- Preston, G. W. 1974, *ARA&A*, 12, 257
- Przybilla, N., & Butler, K. 2001, *A&A*, 379, 955
- Rentzsch-Holm, I. 1996, *A&A*, 305, 275
- Richer, J., Michaud, G., & Turcotte, S. 2000, *ApJ*, 529, 338
- Roby, S. W., & Lambert, D. L. 1990, *ApJS*, 73, 67
- Royer, F., et al. 2014, *A&A*, 562, A84
- Savanov, L. S. 1995, *Astron. Lett.*, 21, 684
- Takeda, Y. 1992a, *PASJ*, 44, 309
- Takeda, Y. 1992b, *PASJ*, 44, 649
- Takeda, Y. 1994, *PASJ*, 46, 53
- Takeda, Y. 1995, *PASJ*, 47, 287
- Takeda, Y. 2003, *A&A*, 402, 343
- Takeda, Y., et al. 2005a, *PASJ*, 57, 13
- Takeda, Y., Han, I., Kang, D.-I., Lee, B.-C., & Kim, K.-M. 2008, *JKAS*, 41, 83 (T08)
- Takeda, Y., Kang, D.-I., Han, I., Lee, B.-C., & Kim, K.-M. 2009, *PASJ*, 61, 1165 (T09)
- Takeda, Y., Kang, D.-I., Han, I., Lee, B.-C., Kim, K.-M., Kawanomoto, S., & Ohishi, N. 2012, *PASJ*, 64, 38
- Takeda, Y., Kawanomoto, S., & Ohishi, N. 2007, *PASJ*, 59, 245
- Takeda, Y., Kawanomoto, S., & Ohishi, N. 2014, *PASJ*, 66, 23
- Takeda, Y., Ohkubo, M., Sato, B., Kambe, E., & Sadakane, K. 2005b, *PASJ*, 57, 27
- Takeda, Y., & Sadakane, K. 1997, *PASJ*, 49, 367
- Takeda, Y., Takada-Hidai, M., Jugaku, J., Sakaue, A., & Sadakane, K. 1999, *PASJ*, 51, 961
- Talon, S., Richard, O., & Michaud, G. 2006, *ApJ*, 645, 634
- van Leeuwen, F. 2007, *Hipparcos, the New Reduction of the Raw Data*, *Astrophysics and Space Science Library*, Vol. 350 (Berlin: Springer)

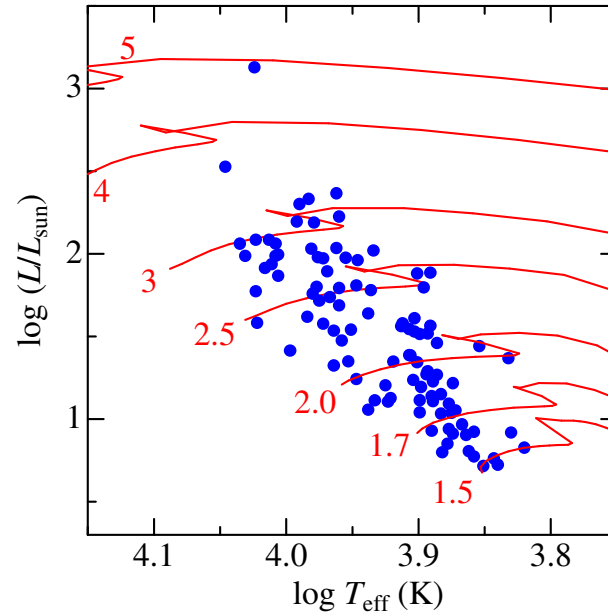


Fig. 1. Our program stars plotted on the theoretical HR diagram ($\log(L/L_{\odot})$ vs. $\log T_{\text{eff}}$), where T_{eff} was derived from colors (cf. section 3) and L was evaluated from visual magnitude (corrected for interstellar extinction; Arenou, Grenon, & Gómez 1992), Hipparcos parallax (van Leeuwen 2007), and bolometric correction (Flower 1996). Theoretical solar-metallicity tracks for 7 different masses (1.5, 1.7, 2, 2.5, 3, 4, and $5 M_{\odot}$), which were computed by Lejeune and Schaerer (2001), are also depicted by solid lines for comparison.

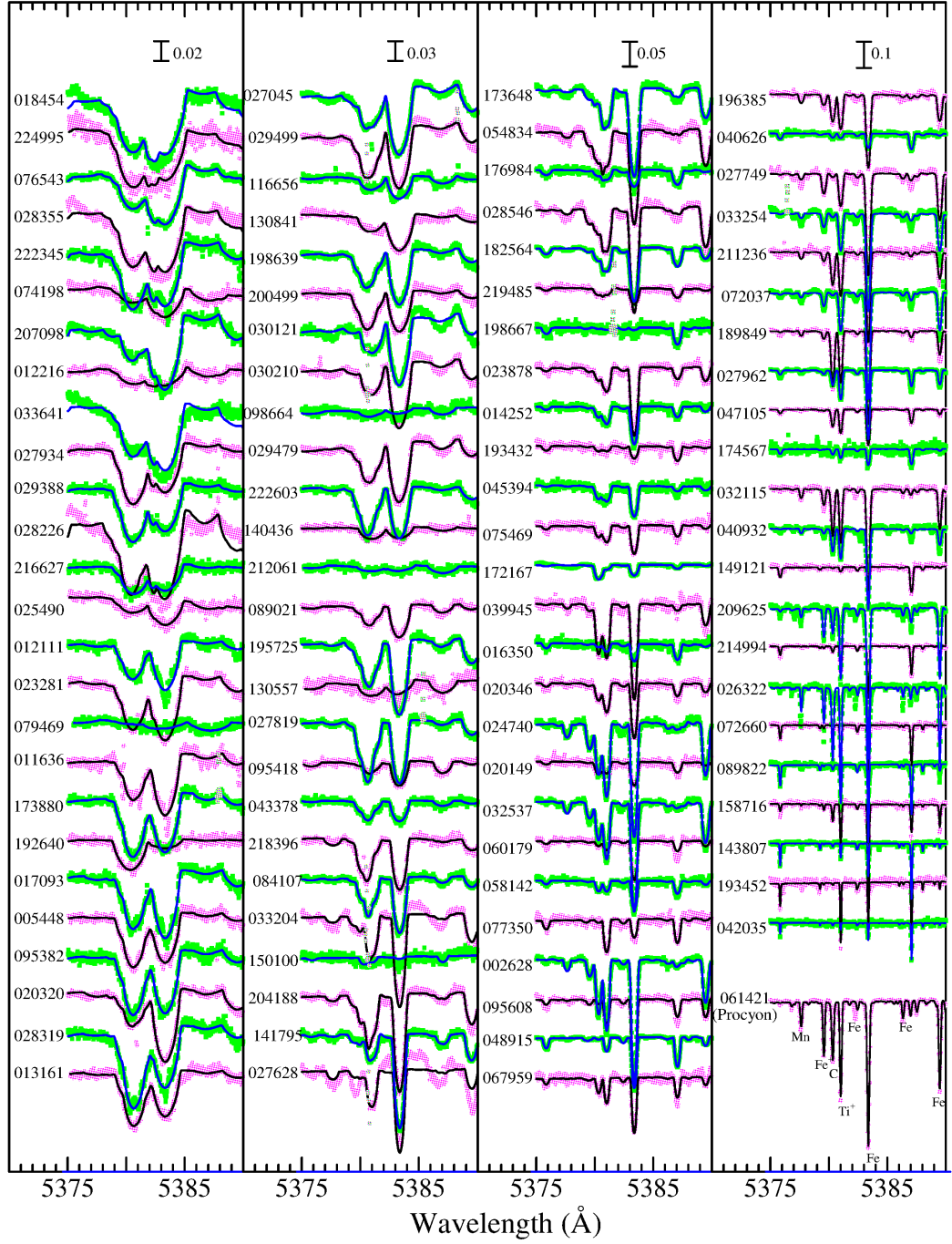


Fig. 2. Synthetic spectrum fitting in the 5375–5390 Å region comprising the C I 5380 line. The best-fit theoretical spectra are shown by solid lines. The observed data are plotted by symbols, where those used in the fitting are colored in pink or green, while those rejected in the fitting (e.g., due to spectrum defect) are depicted in gray. In each panel, the spectra are arranged in the descending order of $v_e \sin i$ as in table 1, and vertical offsets of 0.04, 0.06, 0.08, and 0.15 (from the left to the right panels) are applied to each spectrum (indicated by the HD number) relative to the adjacent one. The case of Procyon (standard star) is displayed at the bottom of the rightmost panel.

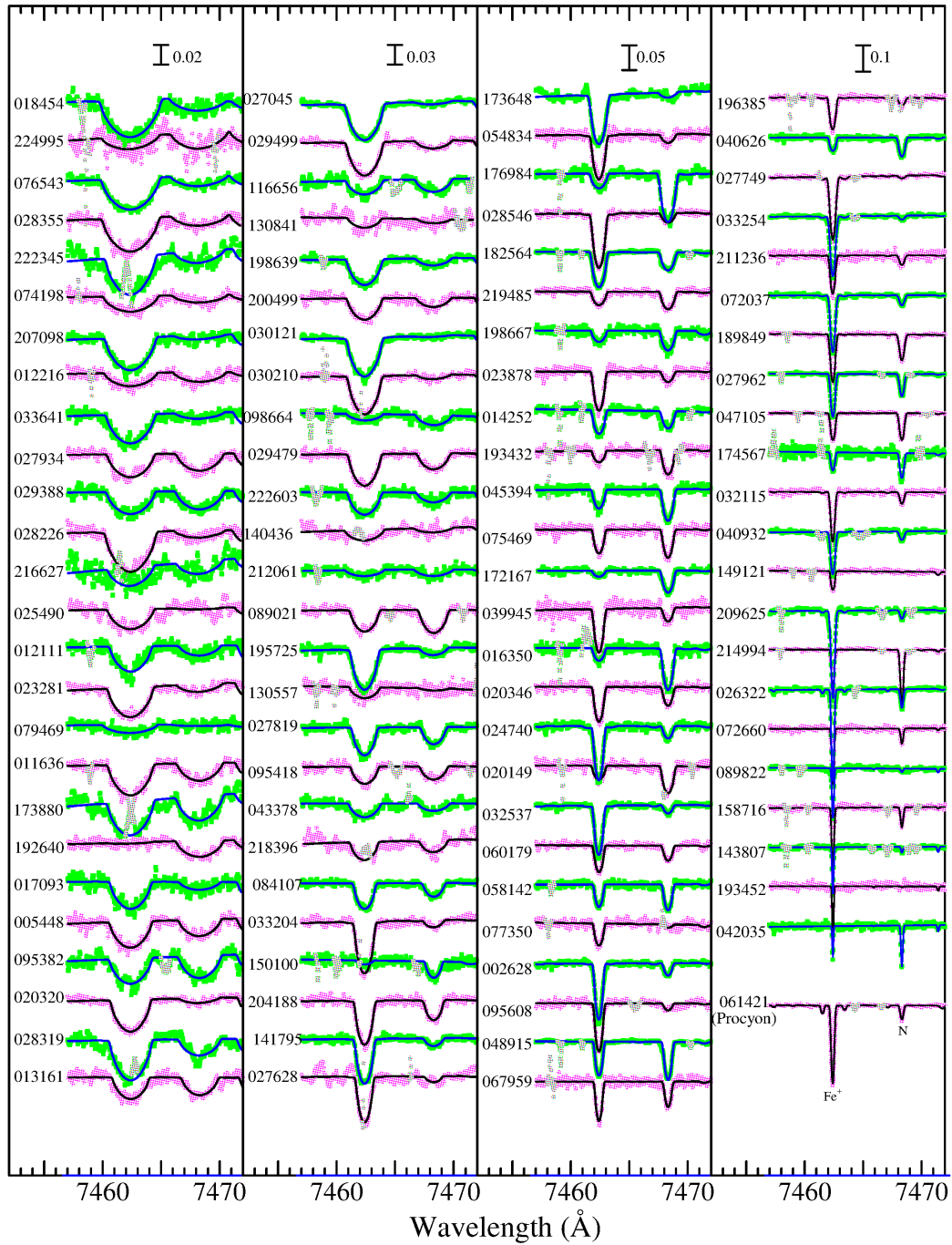


Fig. 3. Synthetic spectrum fitting in the 7457–7472 Å region comprising the N I 7468 line. Otherwise, the same as in figure 2.

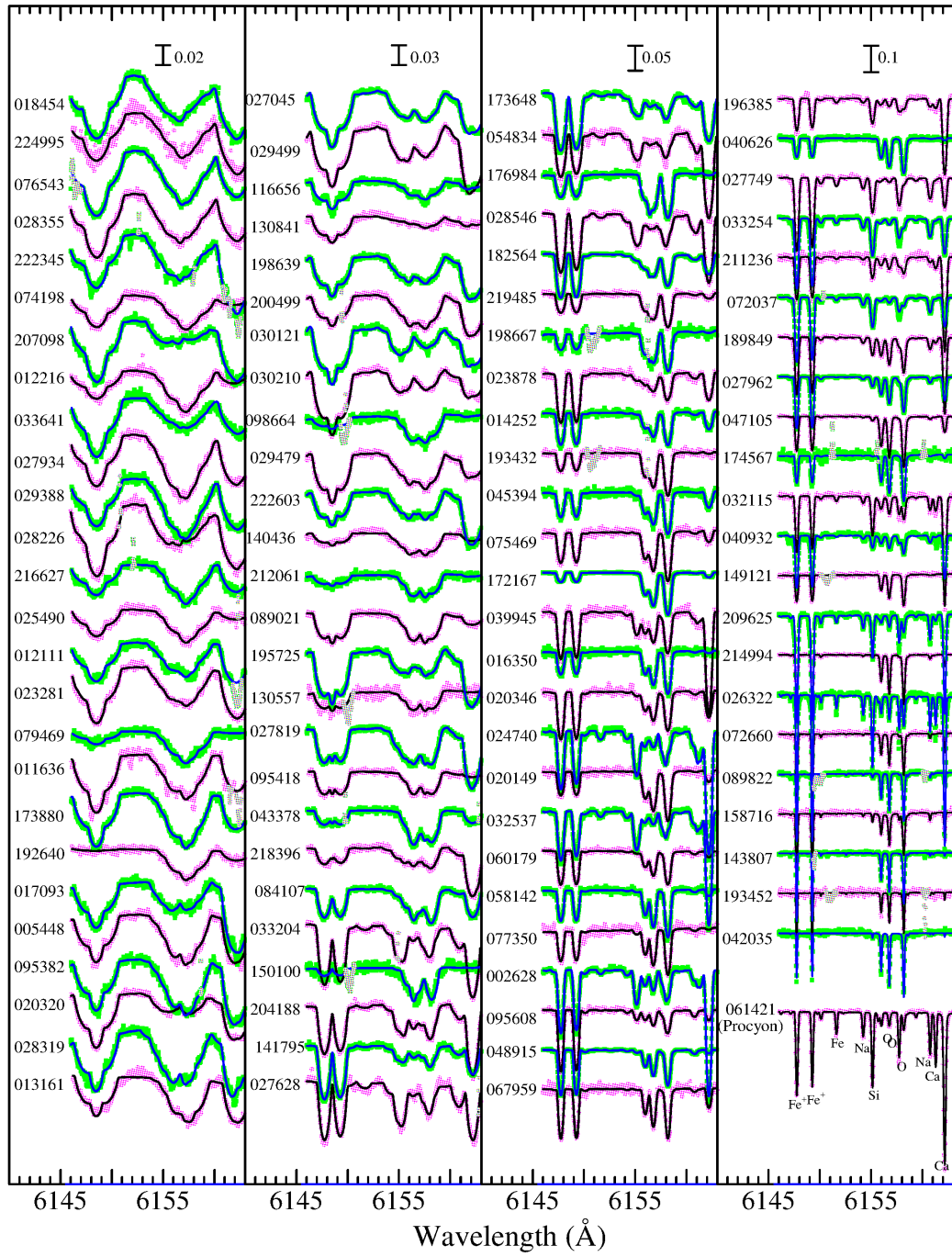


Fig. 4. Synthetic spectrum fitting in the 6146–6163 Å region comprising the O I 6156–8 line. Otherwise, the same as in figure 2.

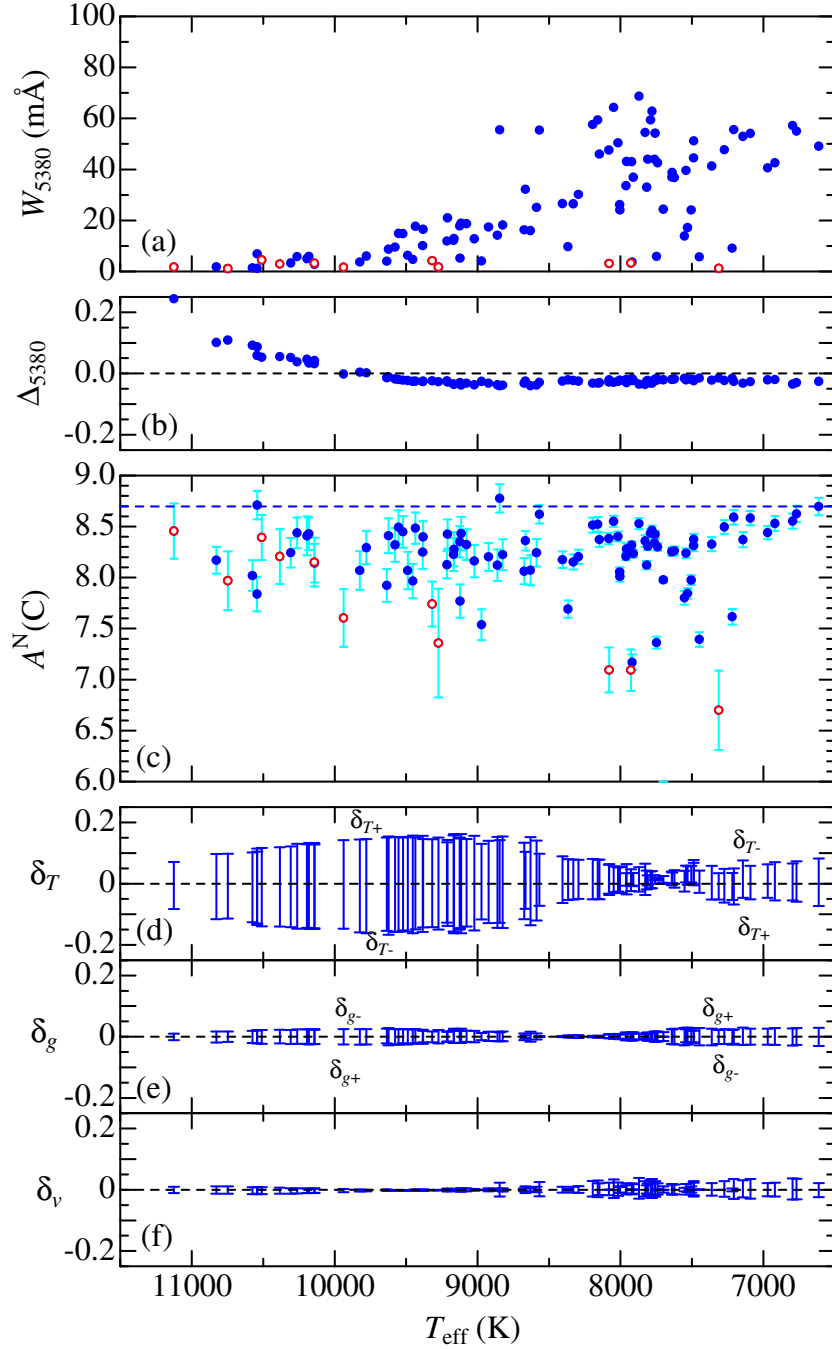


Fig. 5. Carbon abundance and C I 5380-related quantities plotted against T_{eff} . (a) W_{5380} (equivalent width of C I 5380), (b) Δ_{5380} (non-LTE correction for C I 5380), (c) $A^N(\text{C})$ (non-LTE abundance derived from C I 5380) where the error bar denotes δ_{TgW} (cf. subsection 4.3), (d) δ_{T+} and δ_{T-} (abundance variations in response to T_{eff} changes of +3% and -3%), (e) δ_{g+} and δ_{g-} (abundance variations in response to $\log g$ changes by +0.1 dex and -0.1 dex), and (f) δ_{v+} and δ_{v-} (abundance variations in response to perturbing the v_t value by +30% and -30%). The data shown in open circles in panels (a) and (c) denote uncertain results (which had better be regarded rather as upper limits) because of the weakness of lines (cf. subsection 4.3). The abundance of Procyon, which is adopted as the reference, is indicated by the horizontal dashed line in panel (c).

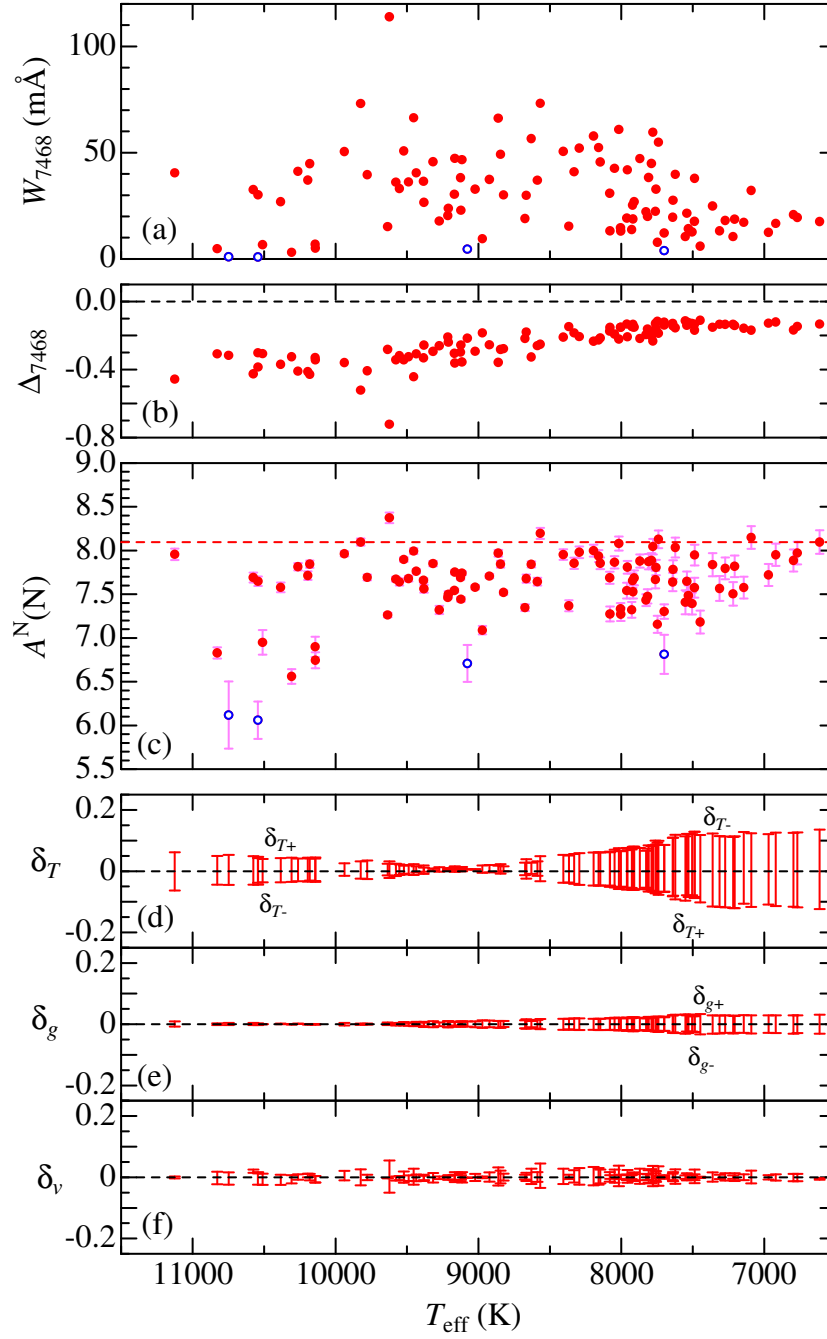


Fig. 6. Nitrogen abundance and N I 7468-related quantities plotted against T_{eff} . Otherwise, the same as in figure 5.

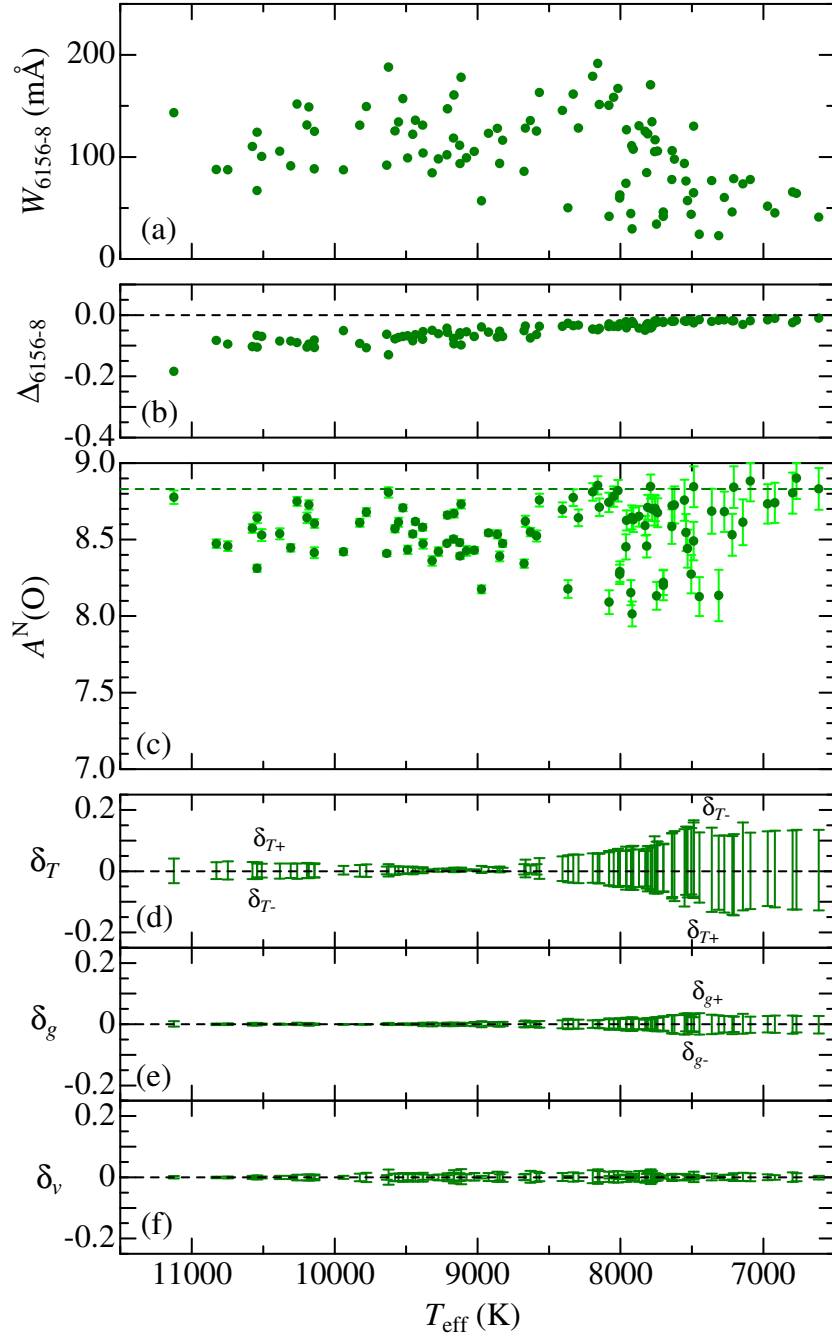


Fig. 7. Oxygen abundance and O I 6156–8-related quantities plotted against T_{eff} . Otherwise, the same as in figure 5.

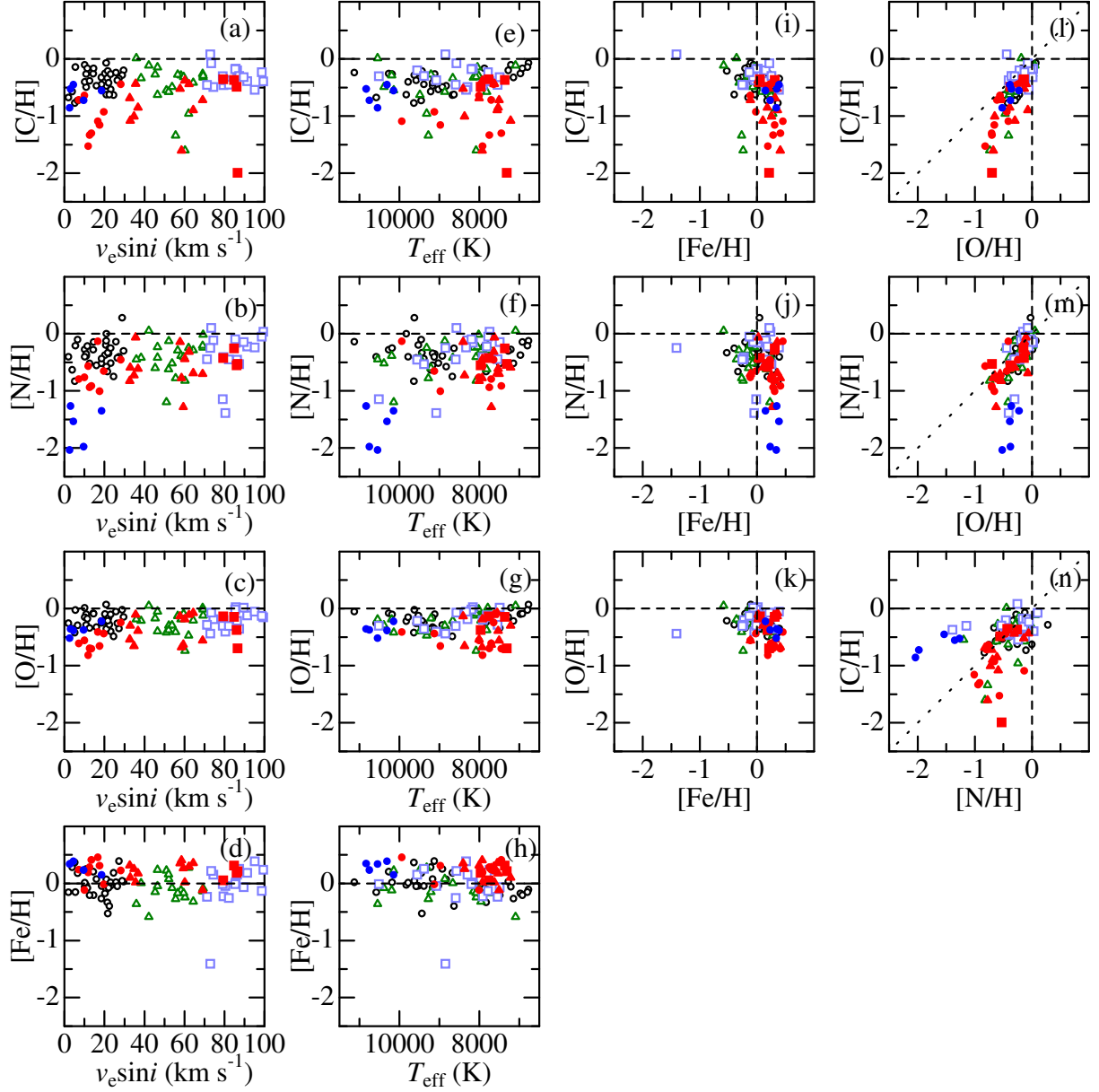


Fig. 8. Graphical display of how the abundances of C, N, and O (relative to Procyon) derived for 100 program stars depend upon $v_e \sin i$ or T_{eff} and how they are mutually related with each other. In the 8 panels on the left-hand side are plotted [C/H], [N/H], [O/H], and [Fe/H] against $v_e \sin i$ (panels a–d) and T_{eff} (panels e–h), while the 6 panels on the right-hand side show the correlation plot for any combination between [C/H], [N/H], [O/H], and [Fe/H] (panels i–n). Stars of different $v_e \sin i$ classes are discriminated by the types of symbols: circles ($0 < v_e \sin i < 30$ km s⁻¹), triangles ($30 \leq v_e \sin i < 70$ km s⁻¹), and squares ($70 \leq v_e \sin i < 100$ km s⁻¹). Those stars classified as chemically peculiar are highlighted by filled symbols: red-filled symbols for Am stars and blue-filled ones for HgMn stars.

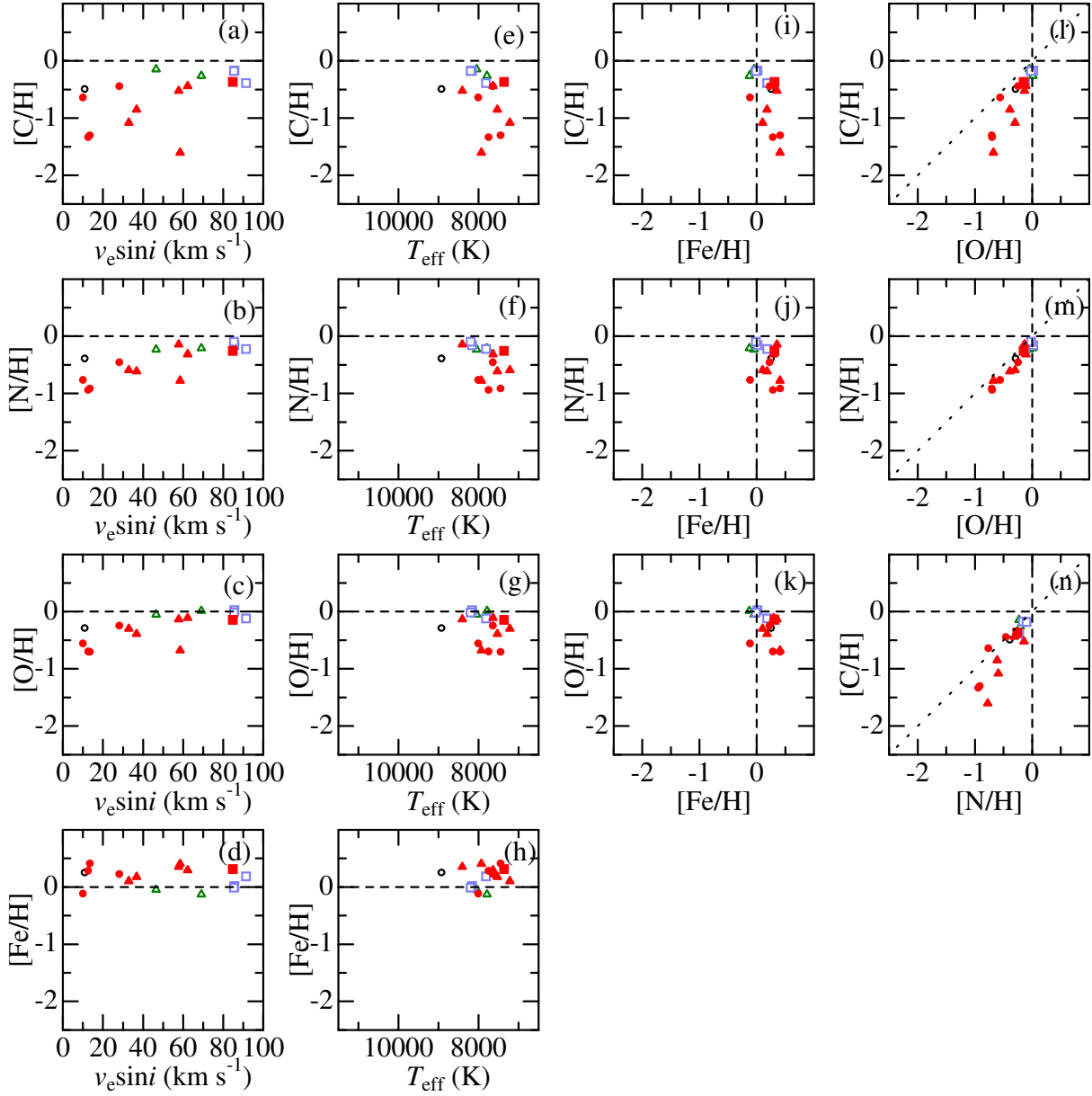


Fig. 9. Graphical display of how the abundances of C, N, and O (relative to Procyon) derived for 16 Hyades stars depend upon $v_e \sin i$ or T_{eff} and how they are mutually related with each other. Otherwise, the same as in figure 8.

Table 1. Stellar parameters and the resulting abundances of the program stars.

| HD# (1) | Name (2) | Sp.Type (3) | T_{eff} (4) | $\log g$ (5) | v_t (6) | $v_e \sin i$ (7) | [Fe/H] (8) | [C/H] (9) | [N/H] (10) | [O/H] (11) | Group (12) | Remark (13) |
|------------|----------------|----------------|-------------------------|-----------------|--------------|---------------------|---------------|--------------|---------------|---------------|---------------|------------------|
| 018454 | 4 Eri | A5IV/V | 7740 | 4.07 | 3.9 | 99.5 | +0.24 | -0.40 | +0.03 | -0.16 | B | V |
| 224995 | 31 Psc | A6V | 7779 | 3.64 | 4.0 | 98.7 | -0.13 | -0.23 | -0.05 | -0.13 | D | V |
| 076543 | σ^1 Cnc | A5III | 8330 | 4.18 | 3.9 | 95.2 | +0.38 | -0.54 | -0.24 | -0.06 | B | SB |
| 028355 | 79 Tau | A7V | 7809 | 3.98 | 4.0 | 91.5 | +0.19 | -0.39 | -0.22 | -0.12 | B | V?, Hyades |
| 222345 | ω^1 Aqr | A7IV | 7487 | 3.88 | 3.8 | 89.7 | -0.07 | -0.32 | -0.15 | +0.01 | B | SB |
| 074198 | γ Cnc | A1IV | 9381 | 4.11 | 2.8 | 87.4 | +0.25 | -0.30 | -0.53 | -0.36 | B | SB |
| 207098 | δ Cap | A5mF2 (IV) | 7312 | 4.06 | 3.6 | 86.6 | +0.21 | (-2.00) | -0.53 | -0.70 | B | SB, Am |
| 012216 | 50 Cas | A2V | 9553 | 3.90 | 2.6 | 86.4 | +0.15 | -0.20 | -0.46 | -0.22 | B | SB2 |
| 033641 | μ Aur | A4m | 7961 | 4.21 | 4.0 | 86.2 | +0.18 | -0.49 | -0.55 | -0.38 | B | V, Am |
| 027934 | κ^1 Tau | A7IV-V | 8159 | 3.84 | 4.0 | 85.7 | +0.02 | -0.17 | -0.16 | +0.02 | B | SB?, Hyades |
| 029388 | 90 Tau | A6V | 8194 | 3.88 | 4.0 | 85.5 | -0.01 | -0.18 | -0.10 | -0.02 | B | SB1, Hyades |
| 028226 | | Am | 7361 | 4.01 | 3.6 | 84.9 | +0.31 | -0.37 | -0.26 | -0.15 | B | SB2, Am, Hyades |
| 216627 | δ Aqr | A3V | 8587 | 3.59 | 3.7 | 82.3 | -0.25 | -0.45 | -0.45 | -0.31 | B | V |
| 025490 | ν Tau | A1V | 9077 | 3.93 | 3.2 | 80.5 | -0.05 | -0.37 | (-1.39) | -0.41 | B | |
| 012111 | 48 Cas | A3IV | 7910 | 4.08 | 4.0 | 79.6 | -0.23 | -0.46 | -0.41 | -0.20 | B | SB |
| 023281 | | A5m | 7761 | 4.19 | 4.0 | 79.4 | +0.05 | -0.36 | -0.43 | -0.14 | B | Am |
| 079469 | θ Hya | B9.5V | 10510 | 4.20 | 1.4 | 79.2 | -0.02 | (-0.30) | -1.15 | -0.30 | B | SB |
| 011636 | β Ari | A5V... | 8294 | 4.12 | 3.9 | 74.5 | +0.15 | -0.49 | -0.12 | -0.19 | B | SB |
| 173880 | 111 Her | A5III | 8567 | 4.27 | 3.8 | 73.5 | +0.22 | -0.08 | +0.10 | -0.07 | B | SB? |
| 192640 | 29 Cyg | A2V | 8845 | 3.86 | 3.5 | 73.0 | -1.41 | +0.08 | -0.25 | -0.44 | B | V |
| 017093 | 38 Ari | A7III-IV | 7541 | 3.95 | 3.8 | 71.3 | -0.23 | -0.46 | -0.45 | -0.29 | B | V |
| 095382 | 59 Leo | A5III | 8017 | 3.95 | 4.0 | 69.3 | -0.09 | -0.29 | -0.02 | -0.01 | B | |
| 005448 | μ And | A5V | 8147 | 3.82 | 4.0 | 69.3 | -0.14 | -0.32 | -0.24 | -0.12 | B | |
| 028319 | θ^2 Tau | A7III | 7789 | 3.68 | 4.0 | 69.1 | -0.13 | -0.26 | -0.21 | +0.01 | B | SB1, Hyades |
| 020320 | ζ Eri | A5m | 7505 | 3.91 | 3.8 | 69.1 | -0.12 | -0.72 | -0.70 | -0.56 | B | SB, Am |
| 027045 | ω^2 Tau | A3m | 7552 | 4.26 | 3.8 | 64.4 | +0.36 | -0.89 | -0.69 | -0.07 | B | SB, Am |
| 013161 | β Tri | A5III | 7957 | 3.68 | 4.0 | 64.4 | -0.32 | -0.42 | -0.29 | -0.21 | B | SB2 |
| 029499 | | A5m | 7638 | 4.08 | 3.9 | 62.3 | +0.29 | -0.44 | -0.31 | -0.11 | B | V, Am, Hyades |
| 116656 | ζ UMa | A2V | 9317 | 4.10 | 2.9 | 62.1 | +0.28 | (-0.96) | -0.25 | -0.47 | B | SB2 |
| 130841 | α^2 Lib | A3IV | 8079 | 3.96 | 4.0 | 60.3 | -0.24 | (-1.60) | -0.82 | -0.74 | B | SB |
| 198639 | 56 Cyg | A4me... | 7921 | 4.09 | 4.0 | 60.2 | +0.02 | -0.38 | -0.44 | -0.19 | B | V?, Am |
| 200499 | η Cap | A5V | 8081 | 3.95 | 4.0 | 59.6 | -0.17 | -0.31 | -0.41 | -0.09 | B | V |
| 030121 | 4 Cam | A3m | 7700 | 3.98 | 3.9 | 59.4 | +0.27 | ... | (-1.28) | -0.63 | B | Am |
| 030210 | | Am... | 7927 | 3.94 | 4.0 | 58.5 | +0.40 | (-1.60) | -0.77 | -0.68 | B | SB1?, Am, Hyades |
| 098664 | σ Leo | B9.5Vs | 10194 | 3.75 | 1.8 | 58.3 | -0.12 | -0.29 | -0.38 | -0.19 | C | SB |
| 029479 | σ^1 Tau | A4m | 8406 | 4.14 | 3.9 | 57.8 | +0.35 | -0.52 | -0.14 | -0.14 | B | SB, Am, Hyades |
| 222603 | λ Psc | A7V | 7757 | 3.99 | 4.0 | 56.6 | -0.17 | -0.27 | -0.29 | -0.13 | B | SB |
| 140436 | γ CrB | A1Vs | 9274 | 3.89 | 3.0 | 55.6 | -0.27 | (-1.34) | -0.78 | -0.41 | B | |
| 212061 | γ Aqr | A0V | 10384 | 3.95 | 1.5 | 53.8 | -0.08 | (-0.49) | -0.52 | -0.29 | B | SB |
| 089021 | λ UMa | A2IV | 8861 | 3.61 | 3.5 | 52.2 | +0.08 | -0.57 | -0.13 | -0.30 | B | V |
| 195725 | θ Cep | A7III | 7816 | 3.74 | 4.0 | 52.1 | +0.16 | -0.57 | -0.62 | -0.37 | B | SB2 |
| 130557 | | B9Vsvar... | 10142 | 3.85 | 1.8 | 51.0 | +0.23 | (-0.55) | -1.20 | -0.42 | C | |
| 095418 | β UMa | A1V | 9489 | 3.85 | 2.7 | 46.5 | +0.24 | -0.63 | -0.42 | -0.40 | B | SB |
| 027819 | δ^2 Tau | A7V | 8047 | 3.95 | 4.0 | 46.5 | -0.05 | -0.15 | -0.23 | -0.05 | B | SB, Hyades |
| 043378 | 2 Lyn | A2Vs | 9210 | 4.09 | 3.0 | 45.3 | -0.15 | -0.27 | -0.60 | -0.17 | B | V? |
| 218396 | | A5V | 7091 | 4.06 | 3.3 | 42.2 | -0.59 | -0.11 | +0.05 | +0.05 | B | |
| 084107 | 15 Leo | A2IV | 8665 | 4.31 | 3.7 | 38.3 | +0.01 | -0.34 | -0.42 | -0.21 | B | |
| 033204 | | A5m | 7530 | 4.06 | 3.8 | 36.8 | +0.18 | -0.85 | -0.61 | -0.39 | B | Am, Hyades |
| 150100 | 16 Dra | B9.5Vn | 10542 | 3.84 | 1.4 | 35.9 | -0.36 | +0.01 | -0.45 | -0.19 | C | V |
| 204188 | | A8m | 7622 | 4.21 | 3.9 | 35.6 | +0.02 | -0.43 | -0.06 | -0.11 | B | SB, Am |
| 141795 | ϵ Ser | A2m | 8367 | 4.24 | 3.9 | 34.8 | +0.25 | -1.01 | -0.73 | -0.65 | B | V, Am |
| 027628 | 60 Tau | A3m | 7218 | 4.05 | 3.5 | 32.9 | +0.10 | -1.08 | -0.59 | -0.30 | B | SB1, Am, Hyades |
| 173648 | ζ^1 Lyr | Am | 8004 | 3.90 | 4.0 | 32.6 | +0.32 | -0.69 | -0.82 | -0.54 | B | SB1, Am |
| 054834 | | A9V | 7273 | 4.21 | 3.5 | 29.6 | +0.03 | -0.20 | -0.30 | -0.15 | D | |
| 176984 | 14 Aql | A1V | 9623 | 3.42 | 2.5 | 28.9 | +0.04 | -0.29 | +0.28 | -0.02 | D | V? |
| 028546 | 81 Tau | Am | 7640 | 4.17 | 3.9 | 28.2 | +0.23 | -0.44 | -0.46 | -0.25 | B | V?, Am, Hyades |
| 182564 | π Dra | A2IIIs | 9125 | 3.80 | 3.1 | 27.3 | +0.39 | -0.35 | -0.41 | -0.35 | A | |
| 219485 | | A0V | 9577 | 3.81 | 2.5 | 26.5 | -0.05 | -0.38 | -0.42 | -0.26 | D | |
| 198667 | 5 Aqr | B9III | 11125 | 3.42 | 0.9 | 25.8 | +0.02 | (-0.24) | -0.14 | -0.05 | C | V |
| 023878 | τ^7 Eri | A1V | 8674 | 3.80 | 3.7 | 24.6 | +0.18 | -0.63 | -0.75 | -0.49 | D | V? |
| 014252 | 10 Tri | A2V | 9023 | 3.64 | 3.3 | 23.2 | -0.04 | -0.53 | -0.52 | -0.40 | D | V |
| 193432 | ν Cap | B9IV | 10180 | 3.91 | 1.8 | 23.1 | +0.02 | -0.27 | -0.25 | -0.10 | D | V? |
| 045394 | 16 Gem | A2Vs | 8630 | 3.42 | 3.7 | 22.5 | -0.40 | -0.62 | -0.25 | -0.28 | D | |
| 075469 | | A2Vs | 9165 | 3.51 | 3.1 | 22.1 | -0.08 | -0.42 | -0.34 | -0.16 | D | |
| 172167 | α Lyr | A0Vvar | 9435 | 3.99 | 2.7 | 21.7 | -0.53 | -0.21 | -0.33 | -0.21 | A | V |
| 039945 | | A5V | 7827 | 3.36 | 4.0 | 21.5 | -0.33 | -0.34 | -0.66 | -0.24 | D | |
| 020346 | | A2IV | 8824 | 3.56 | 3.5 | 21.0 | +0.07 | -0.47 | -0.58 | -0.36 | D | SB? |
| 016350 | | B9.5V | 9824 | 3.72 | 2.2 | 21.0 | -0.03 | -0.63 | +0.00 | -0.22 | D | |
| 024740 | 32 Tau | F2IV | 6768 | 3.77 | 2.7 | 20.9 | -0.11 | -0.07 | -0.12 | +0.07 | D | V |
| 020149 | | A1Vs | 9522 | 3.99 | 2.6 | 20.7 | -0.05 | -0.25 | -0.20 | -0.12 | D | SB? |
| 032537 | 9 Aur | F0V | 6970 | 4.07 | 3.1 | 20.3 | -0.18 | -0.26 | -0.38 | -0.10 | D | SB |
| 060179 | α Gem | A2Vm | 9122 | 3.88 | 3.2 | 19.7 | -0.02 | -0.93 | -0.65 | -0.44 | B | SB1, Am |
| 077350 | ν Cnc | A0III | 10141 | 3.68 | 1.8 | 18.6 | +0.15 | -0.56 | -1.35 | -0.23 | C | SB, HgMn |
| 058142 | 21 Lyn | A1V | 9384 | 3.74 | 2.8 | 18.6 | -0.05 | -0.45 | -0.44 | -0.25 | D | V |
| 002628 | 28 And | A7III | 7143 | 3.48 | 3.3 | 18.5 | -0.27 | -0.32 | -0.52 | -0.22 | D | |
| 095608 | 60 Leo | A1m | 8972 | 4.20 | 3.3 | 17.6 | +0.31 | -1.16 | -1.01 | -0.66 | B | Am |
| 048915 | α CMa | A0m... | 9938 | 4.31 | 2.1 | 16.7 | +0.45 | (-1.09) | -0.13 | -0.41 | A | SB, Am |
| 067959 | | A1V | 9168 | 3.65 | 3.1 | 16.0 | +0.07 | -0.47 | -0.55 | -0.33 | D | |
| 196385 | | A9V | 6919 | 4.23 | 3.0 | 14.6 | -0.21 | -0.17 | -0.15 | -0.09 | D | |
| 040626 | | B9.5IV | 10263 | 4.00 | 1.7 | 14.4 | +0.20 | -0.26 | -0.28 | -0.08 | D | |
| 027749 | 63 Tau | A1m | 7448 | 4.21 | 3.7 | 13.5 | +0.41 | -1.30 | -0.91 | -0.70 | B | SB1, Am, Hyades |
| 211236 | | A8/A9IV/V | 7488 | 3.96 | 3.8 | 12.6 | -0.21 | -0.39 | -0.52 | -0.34 | D | |
| 033254 | 16 Ori | A2m | 7747 | 4.14 | 3.9 | 12.6 | +0.28 | -1.33 | -0.94 | -0.70 | B | SB, Am, Hyades |
| 072037 | 2 UMa | A2m | 7918 | 4.16 | 4.0 | 11.9 | +0.19 | -1.53 | -0.57 | -0.82 | B | Am |
| 189849 | 15 Vul | A4III | 7870 | 3.62 | 4.0 | 11.5 | -0.08 | -0.17 | -0.22 | -0.18 | A | SB |
| 047105 | γ Gem | A0IV | 9115 | 3.49 | 3.2 | 10.9 | -0.03 | -0.27 | -0.35 | -0.10 | A | SB |
| 027962 | δ^3 Tau | A2IV | 8923 | 3.94 | 3.4 | 10.9 | +0.25 | -0.49 | -0.39 | -0.29 | A | SB, Hyades |
| 174567 | | A0Vs | 9778 | 3.59 | 2.3 | 10.2 | +0.01 | -0.40 | -0.40 | -0.15 | D | |
| 032115 | | A8IV | 7207 | 4.13 | 3.4 | 10.1 | -0.06 | -0.11 | -0.28 | +0.01 | D | V |
| 040932 | μ Ori | Am... | 8005 | 3.93 | 4.0 | 10.0 | -0.12 | -0.64 | -0.76 | -0.56 | B | SB1, Am, Hyades |
| 149121 | 28 Her | B9.5III | 10748 | 3.89 | 1.2 | 9.6 | +0.23 | (-0.73) | (-1.98) | -0.37 | C | HgMn |
| 209625 | 32 Aqr | A5m | 7700 | 3.87 | 3.9 | 7.2 | +0.24 | -0.72 | -0.79 | -0.61 | D | SB1, Am |
| 214994 | σ Peg | A1IV | 9453 | 3.64 | 2.7 | 6.6 | +0.18 | -0.73 | -0.10 | -0.30 | A | V |
| 026322 | 44 Tau | F2IV-V | 6795 | 3.46 | 2.8 | 5.5 | -0.15 | -0.14 | -0.21 | -0.03 | D | |
| 072660 | | A1V | 9635 | 3.97 | 2.5 | 5.2 | +0.37 | -0.77 | -0.83 | -0.42 | D | |
| 089822 | | A0sp... | 10307 | 3.89 | 1.6 | 4.5 | +0.39 | -0.45 | -1.54 | -0.39 | C | SB2, HgMn |

Table 1. (Continued)

| HD# (1) | Name (2) | Sp.Type (3) | T_{eff} (4) | $\log g$ (5) | v_t (6) | $v_e \sin i$ (7) | [Fe/H] (8) | [C/H] (9) | [N/H] (10) | [O/H] (11) | Group (12) | Remark (13) |
|------------|-------------|----------------|-------------------------|-----------------|--------------|---------------------|---------------|--------------|---------------|---------------|---------------|----------------|
| 158716 | | A1V | 9214 | 4.30 | 3.0 | 3.9 | +0.28 | -0.57 | -0.63 | -0.36 | D | |
| 143807 | ι CrB | A0p... | 10828 | 4.06 | 1.1 | 3.1 | +0.35 | -0.53 | -1.27 | -0.36 | D | SB, HgMn |
| 193452 | | B9.5III/IV | 10543 | 4.15 | 1.4 | 2.6 | +0.34 | -0.86 | (-2.04) | -0.52 | C | SB1, HgMn |
| 042035 | | B9V | 10575 | 3.82 | 1.4 | 2.0 | -0.16 | -0.68 | -0.40 | -0.26 | D | V |
| 061421 | Procyon | F5IV-V | 6612 | 4.00 | 2.0 | 6.7 | 7.47 | 8.70 | 8.10 | 8.83 | E | SB |

(1) HD number. (2) Bayer/Flamsteed name. (3) Spectral type taken from Hipparcos catalogue (ESA 1997). (4) Effective temperature (in K). (5) Logarithm of surface gravity ($\log g$ in dex, where g is in unit of cm s^{-2}). (6) Microturbulent velocity (in km s^{-1}). (7) Projected rotational velocity (in km s^{-1}) derived from 6146–6163 Å fitting. (8)–(11) Abundances of Fe (from 6146–6163 Å fitting), C, N, and O relative to the standard star Procyon ($[X/H] \equiv A_X(\text{star}) - A_X(\text{Procyon})$), where the parenthesized values denote uncertain results (which may as well be regarded as representing the upper limits). The $A_X^N(\text{Procyon})$ itself is shown in the last row for Procyon, where A is the logarithmic number abundance relative to H expressed in the usual normalization of $A_H = 12$. (12) Group of the data source (cf. table 2). (13) Specific remark [spectroscopic binary (SB) or radial velocity variable (V), chemical peculiarity type (Am or HgMn), membership of Hyades cluster (H); see section 2].

Table 2. Basic information of the adopted observational data.

| Group | # Instr. | Obs. Time | Resolution | Number | Star Type | Reference |
|-------|----------|------------------------|------------|--------|--------------------------|----------------------------|
| †A | HIDES | 2008 Oct | 100000 | 7 | sharp-line A | Takeda et al. (2012) |
| B | BOES | 2008 Jan/Sep, 2009 Jan | 45000 | 56 | sharp/broad-line A | Takeda et al. (2008, 2009) |
| C | HIDES | 2012 May | 70000 | 8 | sharp-line late B | Takeda et al. (2014) |
| D | HIDES | 2017 Aug/Nov | 100000 | 29 | sharp-line early F and A | This study (cf. section 2) |
| *E | HIDES | 2001 Feb | 70000 | 1 | Procyon | Takeda et al. (2005a) |

† Only for HD 172167 (Vega), we adopted the OAO/HIDES spectra of high-S/N (~ 2000) and high-resolution (~ 100000) published by Takeda, Kawanomoto, and Ohishi (2007).

* Regarding the Procyon spectra used for 7457–7472 Å fitting, we used the data published by Allende Prieto et al. (2004).

HIDES and BOES denote “High Dispersion Echelle Spectrograph” at Okayama Astrophysical Observatory and “Bohunsan Observatory Echelle Spectrograph” at Bohunsan Optical Astronomy Observatory, respectively.

Table 3. Outline of spectrum-fitting analysis in this study.

| Purpose | fitting range (Å) | abundances varied* | atomic data source | figure |
|-----------------------------|-------------------|--------------------|--------------------|----------|
| C abundance from C I 5380 | 5375–5390 | C, Ti, Fe | KB95m1 | figure 2 |
| N abundance from N I 7468 | 7457–7472 | N, Fe | KB95m2 | figure 3 |
| O abundance from O I 6156–8 | 6146–6163 | O, Na, Si, Ca, Fe | KB95 | figure 4 |

* The abundances of all other elements than these were fixed in the fitting.

KB95m1 — All the atomic line data presented in Kurucz and Bell (1995) were used, excepting that the contribution of Fe I 5382.474 ($\chi_{\text{low}} = 4.371$ eV) was neglected (because we found its gf value to be erroneously too large).

KB95m2 — All the atomic line data were taken from Kurucz and Bell (1995), excepting that the contribution of S I 7468.588 ($\chi_{\text{low}} = 7.867$ eV) was neglected (because we found its gf value to be erroneously too large).

KB95 — All the atomic line data given in Kurucz and Bell (1995) were used unchanged.

Table 4. Adopted atomic data of relevant CNO lines.

| Line | Multiplet No. | Equivalent Width | λ (Å) | χ_{low} (eV) | $\log gf$ (dex) | Gammar (dex) | Gammass (dex) | Gammaw (dex) |
|------------------------------|---------------|------------------|---------------|--------------------------|-----------------|--------------|---------------|--------------|
| C I 5380 | (11) | W_{5380} | 5380.337 | 7.685 | -1.842 | (7.89) | -4.66 | (-7.36) |
| N I 7468 | (3) | W_{7468} | 7468.312 | 10.336 | -0.270 | 8.64 | -5.40 | (-7.60) |
| O I 6156–8 (9 components) | (10) | W_{6156-8} | 6155.961 | 10.740 | -1.401 | 7.60 | -3.96 | (-7.23) |
| | | | 6155.971 | 10.740 | -1.051 | 7.61 | -3.96 | (-7.23) |
| | | | 6155.989 | 10.740 | -1.161 | 7.61 | -3.96 | (-7.23) |
| | | | 6156.737 | 10.740 | -1.521 | 7.61 | -3.96 | (-7.23) |
| | | | 6156.755 | 10.740 | -0.931 | 7.61 | -3.96 | (-7.23) |
| | | | 6156.778 | 10.740 | -0.731 | 7.62 | -3.96 | (-7.23) |
| | | | 6158.149 | 10.741 | -1.891 | 7.62 | -3.96 | (-7.23) |
| | | | 6158.172 | 10.741 | -1.031 | 7.62 | -3.96 | (-7.23) |
| | | | 6158.187 | 10.741 | -0.441 | 7.61 | -3.96 | (-7.23) |

Following columns 3–5 (laboratory wavelength, lower excitation potential, and gf value), three kinds of damping parameters are presented in columns 6–8: Gammar is the radiation damping width (s^{-1}) [$\log \gamma_{\text{rad}}$], Gammass is the Stark damping width (s^{-1}) per electron density (cm^{-3}) at 10^4 K [$\log(\gamma_e/N_e)$], and Gammaw is the van der Waals damping width (s^{-1}) per hydrogen density (cm^{-3}) at 10^4 K [$\log(\gamma_w/N_H)$].

All the data were taken from Kurucz and Bell (1995), except for the parenthesized damping parameters (unavailable in their compilation), for which the default values computed by the WIDTH9 program were assigned.